Geography of soil contamination for characterization and precision remediation of potentially contaminated sites

Giuliano Langella,[1,2] Antonietta Agrillo,[1] Angelo Basile,[2,3] Roberto De Mascellis,[2,3] Piero Manna,[2,3] Pierpaolo Moretti,[1] Florindo Antonio Mileti,[1] Fabio Terribile,[1,2] Simona Vingiani[1,2]

[1]Dipartimento di Agraria, Università degli Studi di Napoli Federico II, Portici (NA); [2]Centro di Ricerca Interdipartimentale sulla "Earth Critical Zone" per il supporto alla gestione del paesaggio e dell'agroambiente, Università degli Studi di Napoli Federico II, Portici (NA); [3]CNR-ISAFOM, Istituto per i sistemi Agricoli e Forestali del Mediterraneo, Ercolano (NA), Italy

Abstract

One of the fundamental problems experienced when evaluations are required (*e.g.* for reclamation, phytoremediation, containment, *etc*.) on agricultural or industrial contaminated sites is the geospatial variability of pollutants. The general lack of ex-ante information on type, quantity, and location of potentially hazardous substances requires the use of proper investigation tools to identify their spatial distribution. In this work we focused on developing and applying an integrated approach based on the following steps: i) preliminary investigations (analysis of aerial photos from different periods of time); ii) indirect investigations (by geophysical and spectrometric methods such as ARP, DUAL-EM, Profiler, Gamma-ray and X-ray fluorescence); iii) direct investigations (pedological and micromorphological); iv) stochastic modelling and critical risk of chemical concentrations being exceeded. The investigated area is located in the region of Campania (southern Italy), close to the main regional volcanic districts (Phlegraean Fields and Somma-Vesuvius). Maps of the apparent electrical resistivity and conductivity, as well as that of the gamma-ray dose, were obtained for the site in question. On analysing the maps, a good correspondence was found among the outputs obtained from measurements at depths between 0 and 2 m, with a spatial resolution that is slightly better for ARP. The procedure of Normalized Sum of Relative Differences on Geophysical Covariates (NSRDGC) was applied to the 15 maps in order to obtain an integrated variability map of all the surveyed anomalies using the proximal sensors. The resulting map identified the most homogeneous areas where five soil profiles and eight trenches were dug. Field morphological observations enabled three different types of anthropogenic materials enriched in Cr and Zn to be identified. According to their morphology in depth, these materials were not emplaced in a single event. Earth movement and landfilling were carried out at several times in the same area, where a mix of contaminated materials and natural soil is found in the first metre, whereas organic materials are visible separately, probably as a consequence of separate excavations and landfill. Soil micromorphology observations evidenced the presence of Cr-enriched organic materials and secondary crystalline gypsum minerals as well as organic matter coatings inside pores. Such observations suggest the possible fate of some contaminants, highlighting soil mineral and organic associations, as well as the presence of pedofeatures indicating downward movement of colloidal materials.

Correspondence: Vingiani Simona, Dipartimento di Agraria e Centro di Ricerca Interdipartimentale sulla "Earth Critical Zone" per il supporto alla gestione del paesaggio e dell'agroambiente, Università degli Studi di Napoli Federico II, Via Università 100, 80055 Portici (NA), Italy.
E-mail: simona.vingiani@unina.it

Key words: Soil property variation; proximal sensing; electrical resistivity; soil mapping; soil contamination.

Italian Journal of Agronomy 2018; 13(s1):6-15

Introduction

Soil spatial variability is a key issue for land management both in agriculture (*e.g.* precision farming) (Corwin and Lesch, 2003; Mzuku *et al.,* 2005; Aggelopoulou *et al.,* 2010; 2011; Fulton *et al.,* 2011) and in other environmental contexts (*e.g.* contaminated sites) (da Silva *et al.,* 2017; Wang *et al.,* 2017; Shaheen and Iqbal, 2018). When contaminated sites are investigated a twofold spatial variability is experienced due to: i) natural spatial variability of soil properties; and ii) anthropogenic spatial variability due to the sources of the contamination. Moreover, the actual spatial distribution of anthropogenic soil contaminants is almost always unknown. This is the case of most industrial sites where the detailed history of contamination is often lost in time. This is due to two main factors: the loss of historic information of industrial land use for each area of a specific industrial site, and its modification over time (*e.g.* placing/removal of materials). This also holds for most illegal waste dumping, for which type/quantity and especially localization of contaminants are unknown.

Given the above considerations, it is evident that in both analysis and subsequent remediation of contaminated sites, this lack of ex-ante information on the geography of contamination (type/quantity/location) requires that proper investigation tools be adopted to achieve an understanding of the spatial distribution of contamination.

This specific contribution aims to focus on how to acquire such detailed knowledge of the spatial distribution of contamination despite the evidence that this is often neglected and ignored. The regulatory criteria to be adopted in Italy in the case of poten-

tial contamination refer to Law Decree 152/06 - Part IV- Title V, according to which a site must be considered potentially contaminated if element concentrations (even only for one element) exceed the established screening values (CSCs). In such cases, environmental characterization of the site has to be performed. Although the law considers the geospatial component of the hypothetical pollution source, its factual application requires a very broad sampling aggregation scheme where *soil surface* refers to a composite sample in the 0-1 m depth range, that could lead to dilute the contaminants, thereby underestimating their concentrations (Rocco *et al*., 2016). According to the law, there are no obligations either for the sampling method to be used (free or systematic) or for the number of sampling points. In many real applications sampling density often refers to the old Decree 471/99 (Annex 2), whereby establishing: i) areas <1 hectare requires at least five sampling points; ii) areas between 1 and 5 ha requires 5 to 15 sampling points; and iii) areas > 5-25 ha requires 15-60 sampling points. These long-established specifications have actually become a standard to which many of the characterization studies of Italian contaminated sites refer. Here we question whether such a small number of observations is really sufficient to define the spatial distribution (in terms of surfaces and depth) of soil contamination. We consider whether the entire site of interest is really contaminated or only parts of it - and also - the extent of this contamination at each detailed location. For the above reasons, here we elaborate a methodological integrated approach, combining many different techniques, aiming to produce a model of contaminant spatial distribution as close as possible to reality.

The approach that we developed is based on the following steps: i) preliminary investigations; ii) indirect investigations; iii) direct investigations; iv) stochastic modelling and critical risk of chemical concentrations exceeded. We considered that almost all geophysical methods are non-destructive, very sensitive and used for describing subsurface properties in engineering, geological, environmental and forensic problems, without digging. There are many methods that differ in the detection of soil physical properties (such as electrical resistivity/conductivity, magnetic susceptibility, velocity of P or S waves). Therefore, the choice of the best method is related to the purpose of prospecting and it is impossible to know in advance which method will perform best. Moreover, such investigations generally enable rapid acquisition of data and can help to transform point-based soil analysis into information on continuous spatial soil properties. Such approaches are already well established in several contexts requiring rapid non-destructive high-resolution soil investigations, such as viticultural zoning at farm scale (Bonfante *et al*., 2015; Tardaguila *et al.*, 2018). For all the above reasons, a geospatial survey, using multi-frequency electromagnetic (EM) conductivity meters (such as Profiler EMP-400 and DUAL-EM), automatic resistivity profiling (ARP) and gamma-ray spectrometry as indirect methods, was carried out in order to acquire knowledge on the geospatial distribution of soil physical properties, like electrical resistivity/conductivity, to be used as proxy for understanding the location of buried waste. The maps obtained and related signal anomaly were processed (using geostatistical methods) and represented the basis for a direct survey focusing on the areas where the highest composite anomaly signals occur. A geophysical anomaly (*i.e.* an area where geophysical properties differ from those of the surrounding areas) is due to differences in soil properties and can thus represent a waste burial site in the surveyed area. Profiles and trenches were dug so as to identify: i) possible relationships between anomalies and waste occurrence; and ii) sampling and analyses of allochthonous/contaminated materials. The body of information thereby obtained enables the spatial nature of contamination to be ascertained as a prerequisite for optimal characterization and remediation of a contaminated site.

Materials and methods

Environmental setting

The investigated area is located at Giugliano in Campania (San Giuseppiello site), in the province of Naples, in Campania (southern Italy). The 60,000 m^2 site consists of farmland which, according to preliminary characterization, was potentially contaminated by Cr, Zn and heavy hydrocarbons (C>12) due to illegal burying of tannery sludge and waste. The field, previously used for fruit orchards and arable crops, is subjected to a phytoremediation programme (Fiorentino *et al.,* 2018).

Geologically, the site is located in the Piana Campana graben, to the North of the Phlegrean Fields and NW of the Somma-Vesuvius complex, which are the main active volcanoes of Campania. In this lowland environment a preferential accumulation of pyroclastic deposits is found (Di Vito *et al.*, 2013; Orsi *et al.*, 2004) due to the proximity to these eruptive centres. Therefore, the soils of the site surroundings are the result of a different extent of andosolization, which gave rise to formation of soils classified as Pachi-Vitric Andosols (di Gennaro *et al.,* 2002) and Hypereutric Cambisols (Aric, Humic, Loamic, Tephric) (Vingiani *et al.,* 2018a; 2018b). These soils are known from the literature for their excellent properties (Nanzyo, 2002; Shoji and Takahashi, 2003; Shoji *et al*., 1993) that give high chemical and physical fertility to ecosystems (Maeda *et al.,* 1977; Quantin, 1990), both in volcanic districts and in non-volcanic mountain landscapes (Mileti *et al.,* 2018; Vingiani *et al*., 2013; Vingiani *et al.,* 2014). In spite of these positive properties, Andosols and andic soils have an inner *fragility* to land degradation and pollution (Kabata-Pendias, 2001; Latrille *et al.,* 2003; Tanneberg *et al*., 2001; Vingiani *et al.,* 2015; Zhao *et al.,* 2006), which renders the investigated area highly vulnerable.

Aerial photo analysis and geophysical prospecting

As the first step, all the existing information (topographic and land use maps, aerial photos, *etc*.) on the site was collected in order to identify recent changes that might help identify anomalies or simple modifications of interest. The periods of interest were those preceding and following waste burial. We analysed the aerial photos obtained from the National Geoportal (WMS services) and Google Earth, considering five years, in the period from 1989 to the present. Then we proceeded with the geospatial surveys, applying geophysical methods. Geophysical modelling provides generalized and non-unique solutions to questions concerning the geometry of natural/anthropogenic soil horizons. The methodological approach applied involves the combined use of several indirect surveys to characterize the site, such as automatic resistivity profiling (ARP) and frequency domain electromagnetic induction (Profilers EMP400 and DUAL-EM 642 S). Among the geophysical tools applied in soil science, electrical methods are considered potentially useful to characterize soil. The ARP technique allows to measure the apparent electrical resistivity of soil. This property is related to the spatial and temporal variability of many other soil physical properties (such as structure, water content or fluid composition). Apparent soil electrical resistivity results from the *combination* of all the soil component resistances in the investigated volume. The ARP equipment was developed by Geocarta SA. It consists in a patented mobile multi-electrode system in which sev-

eral electrodes (eight gear wheels) are automatically inserted into the soil and made to advance (by passive rotation on the soil) during field acquisition (speed <=8 m/s). The distances between the dipoles are 0.5, 1.0 and 1.7 m. In this way it is possible to survey simultaneously a vertical section at three depths. The ARP equipment was towed by a quad and the GPS position for all the measurements was recorded. In addition, electromagnetic induction (EMI) methods in the frequency domain were used to measure the electrical conductivity (the inverse of electrical resistivity) of the subsurface. Two instruments with different characteristics (DUAL-EM 642-S and Profiler EMP-400) were used and acquisition required just one day per technique.

The DUAL-EM 642S induction electromagnetometer (DUAL-EM Inc., Canada) was used with three pairs of sensors arranged in DUAL configuration, separated by 2, 4 and 6 m. Each pair of sensors is able to measure simultaneously at two different depths. Thus DUALEM-642S is able to simultaneously acquire a profile of apparent electrical resistivity (ρa) and apparent magnetic susceptibility (χa) at six different depths and can be configured in two modes: co-planar (HCP) and perpendicular (PRP).

These configurations, which correspond to different measurement depths, make the DUAL-EM-642S very suitable for analysis of both ρa and χa up to 9 m depth. Measurements were made according to parallel profiles with a distance of about 2-4 m.

The Profiler EMP-400 is a portable, digital multi-frequency electromagnetic induction sensor. The user can collect from one (1) to three (3) frequencies simultaneously. The system bandwidth extends from 1 kHz to 16 kHz in 1 kHz steps. The magnitude of the in-phase and quadrature components of the induced secondary field, as well as the apparent conductivity and magnetic susceptibility, are collected and stored for each reading along with a time stamp and GPS data.

Unlike conventional resistivity techniques, with electromagnetic induction sensors no ground contact was required. However, all the systems used allow almost continuous acquisitions to be carried out, with a spacing of about two metres between one row and the next. A single day acquisition was required for each technique. All the available information (maps) was processed in a GIS environment in order to define the areas characterized by anomalies of the signal, greater homogeneity and heterogeneity.

ARP and Profiler EMP-400 data were generally acquired through the parallel profile sampling scheme with 10 cm spacings along the transects, while interfiles between transects ranged between less than 1 m (ARP) to 5-6 m (Profiler).

Another indirect method used, not correlated with those described above, is gamma-ray spectrometry. The gamma-ray spectrometer is designed to measure natural and artificial radioisotopes in the ground. The instrument always measures the complete spectrum, from which it evaluates the cps values in ROIs and calculates the concentrations of elements K [%], eU [ppm] and eTh [ppm]. The natural dose rate (in nGy/h) is calculated from measured concentrations of K, eU and eTh according to IAEA recommendations. The measurements were performed as points and the position of the measured site has been set using external GPS. Using (geo)statistic interpolation it was possible to spatialize the point-based information of K [%], eU [ppm], eTh [ppm] and the natural dose rate (in nGy/h) as was done for resistivity data.

Positioning of soil trenches and profiles

The whole set of observations was crossed using a multivariate statistical approach in order to carry out a rational sampling campaign aimed at complete site characterization. Indeed, the indirect surveys (Profiler, DUAL-EM, ARP, and Gamma-ray) produced a total of 15 information layers as follows: Profiler electrical apparent conductivity at 15 KHz, 10 KHz and 5 KHz; DUAL-EM resistivity at depths 1.0 m, 2.0 m, 3.0 m, 3.2 m, 6.4 m and 9.5 m; ARP resistivity at depths 0.5 m, 1.0 m and 1.7 m; Gamma-ray K [%], eU [ppm] and eTh [ppm].

Each instrument produced a specific density and location of the signal points, for which the data were merged to report all the information on a regular grid at 5 m resolution (high resolution to offset the high density and possible anomalies measured by the instruments). In order to highlight and maximize the global anomaly given by the contribution of all the geophysical sensors, the Normalized Sum of Relative Differences on Geophysical Covariates (NSRDGC) was then calculated as follows:

$$NSRDGC_t = \sum_{i=1}^{15} \sum_{n=1}^{8} \frac{abs(V_t^i - V_n^i)}{V_t^i} \quad (1)$$

for each t target pixel, where V_t^i is the value of the i-th geophysical signal at t target pixel, V_n^i is the value of the i-th geophysical signal at n-th neighbour pixel, n accounts for the 8-adjacent pixels of the target pixel, and i accounts for the list of 15 geophysical signals.

The NSRDGC is calculated on the 1 m resolution grid according to the following steps: i) for each target pixel, a list of 15 values according to the number of sensors and frequencies (*i.e.* auxiliary covariates) is retrieved from the proximal sensing measurements (*e.g.* for signal number two we have V^2_n); ii) for each auxiliary covariate, the list of 8-adjacent pixels to the target pixel is produced and stored in the vector $V^2_{1\ to\ 8}$; iii) the $NSRDGC_t$ at target pixel t is calculated by summing the absolute differences of the target pixel with respect to the 8-adjacent pixels and to the values in the neighbourhood given by the 15 auxiliary covariates. By extending the calculation on the whole regular grid, the hotspot map was generated by aggregating all the collected geophysical signals. Relatively high pixel values are found where an important leap occurred between one point and the points around. This procedure was practical since the resulting map aided identification of the areas in which to dig profiles and trenches, according to the spatial distribution of major and/or minor variations in the data fused information. Eight trenches were located at the major geophysical contrasts in order to identify the spatial variability of the site while five profiles were located in the most homogeneous units. Trench size varied between 4 and 7 m in length, with a depth and width of about 2 m, while the profiles had a length of about 2 m, but with the same depth and width. One or two representative profiles were sampled per trench and a photographic report was also produced for a vertical and horizontal reconstruction of the trenches. For each profile morphological description (FAO, 2006) and undisturbed sampling for micromorphological analyses were also carried out, as well as bulk sampling for further chemical and physical analyses.

XRF and micromorphological analyses

A portable handheld XRF analyzer was used for rapid identification of the materials most contaminated by potentially toxic elements (PTEs) directly in the field in order to address the following soil sampling procedure for assessing PTE content and bioavailability (Rocco *et al.,* 2018). Twenty-one elements (As, Ca, Cd, Cr, Cu, Fe, K, Mn, Nb, Ni, Pb, Rb, Sn, Sr, Th, Ti, U, V, Zn, Zr and Y) were measured on smooth uniform surfaces, with complete contact between instrument and sample surface to minimize surface effects. Scanning was carried out with a Delta Professional (Olympus, DPO-4000) using a large window (8 mm^2). The instrument features a

Ta/Au X-ray tube operating at 15–40 kV with integrated large area silicon drift detector (165 eV). Innov-X software was used in Soil mode, which consists of three beams operating sequentially, with acquisition times of 30 seconds per beam. Then, the most significant materials, in terms of soil contamination, were selected and a total of 35 undisturbed samples were collected from soil trenches and profiles by means of Kubiena boxes (5x10x5 cm). Samples were impregnated with polyester crystic resin and large (10x5x0.003 cm) thin sections were produced using the FitzPatrick methodology (1984, 1993). Thin sections were analysed under optical microscope in plain (PPL) and crossed (XPL) polarized light. XRF analyses were also performed on soil thin sections using a small spot collimator (analysis area of 0.07 cm^2), to have a preliminary assessment of micro-pedofeatures contamination.

Results and discussion

Through the study of the aerial photos, we identified changes in land use (from orchard to arable) in different sites as well as the occurrence of traces of temporary roadways that could well have been caused by the transit of heavy vehicles. The photos in question are shown in Figure 1.

Nevertheless, it is self-evident that these signs of heavy vehicle transit are not helpful for understanding the distribution of contaminants in the area. Indeed, the pictures would be useful only if the illegal spillage was associated with the acquisition of simultaneous remotely sensed images (as in the case of drones). Needless to add, such data are very rare when dealing with illegal activities. Indeed,

Figure 1. Aerial photos of the study area from 1989 to the present day.

waste spill activities are generally carried out very quickly and most often overnight.

Mapping of geophysical properties and gamma-ray spectrometry

The geoelectric, electromagnetic and spectrometric investigations carried out in the surveyed site by ARP, DUAL-EM, Profiler and Gamma-ray spectrometry enabled the mapping of the apparent electrical resistivity and conductivity and gamma-ray dose of the investigated site. Analysing the maps obtained from measurement (surface acquisition scheme in Figure 2) at depths between 0 and 2 m (Figures 3-6), it may be stated that there is good correspondence between the outputs of the various instruments, with a spatial resolution that is slightly better for the ARP. In further detail, maps show that part of the variability of the observed geophysical anomalies can be explained by the different land use that most likely results in different soil moisture and hence the differences observed between the investigated soils. In particular: i) the area with low resistivity located at the W site (shown in blue in Figure 3) has a land use of uncultivated grassland amongst prevailing orchard; ii) the N-S variability of geophysical anomalies, which is evident throughout the survey area, may reflect the arrangement of crop rows.

However, land use cannot explain all the other geophysical anomalies. In particular, long-range variability is clearly shown (Figures 3 and 5) with a large central area showing higher resistivity surrounded by two less resistive areas (of these two only the W area has non-arboreal land use). In addition, within each of these areas there is short-range variability with alternating - apparently chaotic - of highly variable resistivity areas. Moreover, the measurements made with different signal frequencies (*e.g.* the case for DUAL-EM is reported in Figures 4 and 5) and hence with different investigated volumes, highlight results with very different mapping areas, especially when observing short-range variability. For example, in Figure 5 (estimated volume depth: 3 m) there are many geophysical anomalies, completely different from the same survey reported in Figure 4 (estimated volume depth: 1.7 m).

It is evident that *a priori* it is impossible to ascertain the nature (natural *vs* anthropogenic) of such variability occurring among the 15 maps obtained from the different sensors used (Figure 7A). On the basis of the 15 maps we then applied the NSRDGC procedure in order to obtain an integrated map of the variability of all surveyed anomalies obtained by proximal sensors. Reported in Figure 7B the map clearly shows higher variability (larger violet circles) in a N-S direction with a few additional large patches. On the basis

Figure 2. Example of an acquisition path for the ARP technique.

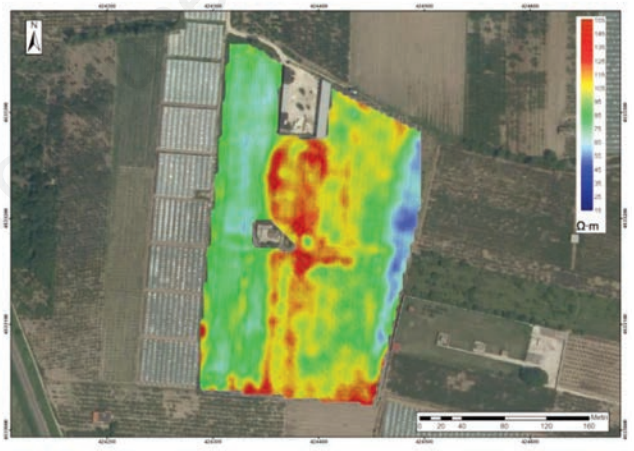

Figure 4. Electrical resistivity map obtained using DUAL-EM (estimated volume depth 1 m).

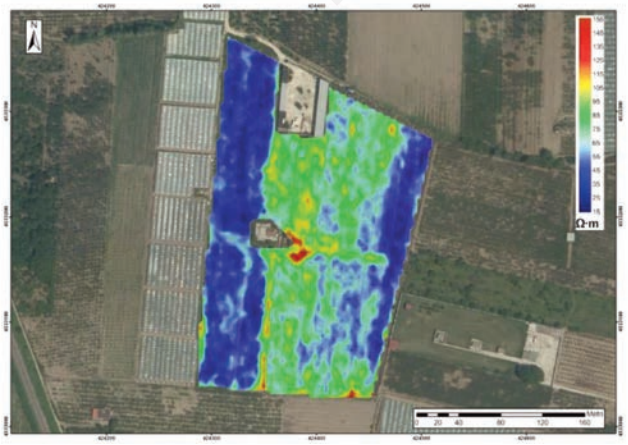

Figure 3. Electrical resistivity map using ARP. Channel 3 - depth: 1.7 m.

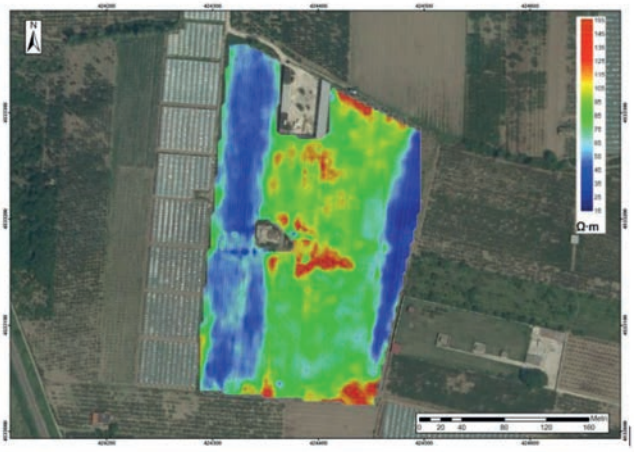

Figure 5. Resistivity map obtained using DUAL-EM (estimated volume depth: 3 m).

of this NSRDGC information, we then located soil profiles in more homogeneous areas and soil trenches in more heterogeneous areas. In so doing, we paid special attention to avoid: i) N-S anomalies due simply to changes in land use; ii) anomalies close to manmade structures (walls, small houses and warehouses, *etc*.); and iii) anomalies already known in the SW portion of the field.

Trenches and profiles

The location of the pedological observations is shown in Figure 8. Soil morphological observations enabled identification of three different types of anthropogenic materials enriched in Cr and Zn: i) coarse material (2-7 cm) and sediments in well-identifiable place of the soil profile, such as in trench 1, where Cr reached a concentration of 2.7%; ii) organic surface material used as *compost* identified in profile 4; material rich in organic component, more or less mineralized, in trenches 2 and 4. Evidence from soil morphology with depth suggests that emplacement of these materials did not take place in a single event, but several earth movements and landfill were carried out in the same area and the effects of these movements were identified from the detailed observation of trenches 2 and 4 (Figure 9). The extreme complexity and variability of the landfill is clearly visible in trench 4, where a mix of pollutants with natural soil is found in the first metre of the central area, whereas organic matter not present in the central part is visible laterally, probably as a consequence of successive excavations. As a general rule, illegal landfills are found in the first two metres, but they also occur at different depths. Indeed, in two of the open trenches (TR2 and TR4) the lower limit of the landfill was not identified and is thus considered to be deeper than 240 cm (bottom of the soil excavation). Further investigation should be carried out to ascertain the depth of the landfill by means of environmental

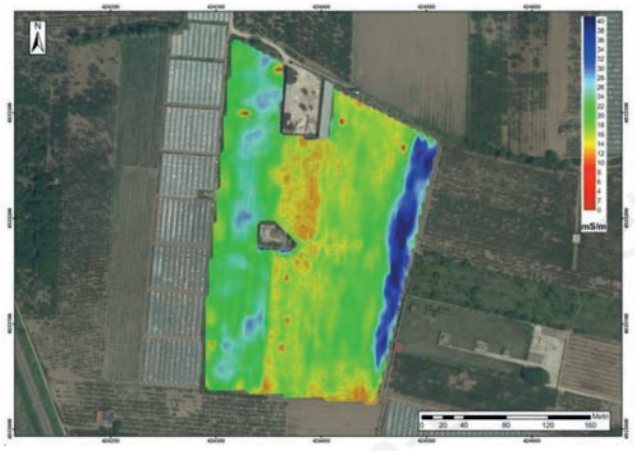

Figure 6. Electrical conductivity obtained using profiler with 15KHz frequency.

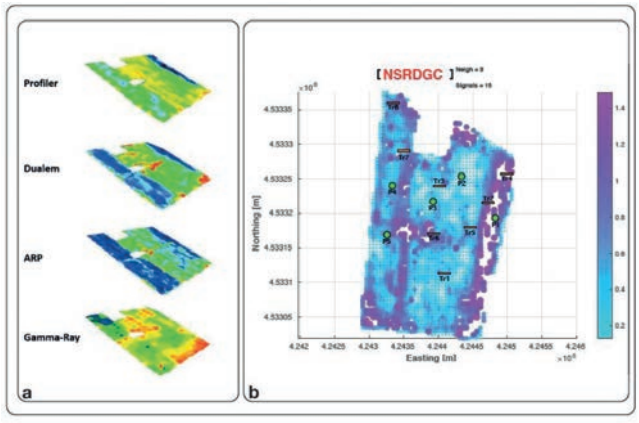

Figure 7. A) Maps obtained from the sensors used; B) map reporting the variability of the normalized sum of relative differences on geophysical covariates (NSRDGC).

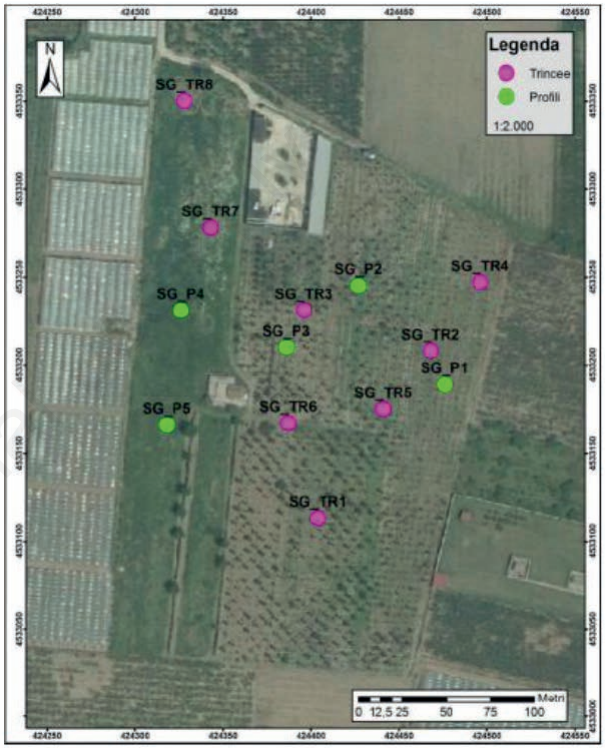

Figure 8. Location of the pedological (trench and profile) observations.

Figure 9. Pictures from trenches 2 and 4.

Figure 10. Picture from trench 3.

core drills. Observations also showed that human impact greatly affected the areas along the field margins whereas within the less disturbed area anthropogenic materials were identified between an abandoned cottage and a shed (trench 3, Figure 10), albeit in smaller amounts and at lower depths compared with the marginal areas. Another less disturbed area was identified in correspondence of profile 2 (Figure 11), which shows signs of anthropic disturbance in the first metre, but starting from 100 cm displays a natural distribution of soil horizons. In this profile two buried soil cycles, typical of volcanic environments, truncated upwards by recent human activities are clearly visible.

Micromorphological analysis

The micromorphological study carried out on thin sections from selected soil horizons enabled the identification of interesting soil pedofeatures. In particular, in one of the most contaminated soils in the TR2: i) blackish aggregates of organic materials standing alone (Figure 12A and B) or mixed with mineral particles (Figure 12C and D); and ii) several carbonate fragments were recognized in deep horizons (175-185 cm). From analysis of the elemental composition (Table 1), the organic materials proved highly enriched in Cr (from 2109 to 3427 mg kg^{-1}), Fe (from 3243 to 4945 mg kg^{-1}), Ca (from 83,907 to 124,982 mg kg^{-1}), S (16,751 to 21,737 mg kg^{-1}) and to a lesser extent Zn (from 92 to 122 mg kg^{-1}), compared with the soil matrix (Table 1 with reference to the light brown soil matrix). Moreover, in many soil pores fine coatings were also identified (Figure 12E and F). As observed, coatings are made by alternate levels of pale yellowish and reddish layers, optically isotropic, indicating downward movements of organic materials with different chemical composition and at different times. Very frequently, acicular small crystals light grey in PPL (Figure 12D and E) and with high interference colours in XPL (Figure 12D and E) were found to be present in association with the organic materials. Due to their small size, general absence in volcanic materials of this environment and their occurrence within organic materials, they were interpreted as minerals of secondary origin. From their composition (Table 1), showing very high content of both S (47,597 mg kg^{-1}) and Ca (80,952 mg kg^{-1}), they were recognized as calcium sulphates and most probably gypsum.

Figure 11. Profile 2, as an example of undisturbed soil.

Table 1. Concentration of selected elements obtained by XRF analyses of soil pedofeatures identified by the micromorphological study.

	Light brown soil matrix 1	Light brown soil matrix 2	Blackish aggregate 1 mg kg^{-1}	Blackish aggregate 2	Carbonate fragments	Acicular crystals
S	1814±474	2686±523	21,737±1288	16,751±1136	3607±717	47,597±1872
K	6902±243	24,187±545	1213±126	2292±154	2229±155	1744±132
Ca	37,231±719	30,028±592	124,982±2180	83,907±1515	123,984±2204	80,952±1441
Ti	414±25	884±37	917±39	967±41	206±21	336±23
V	19±3	29±4	18±4	34±51	5±3	11±3
Cr	37±6	63±7	3427±68	2109±47	22±6	489±17
Mn	113±9	241±12	86±16	73±14	1172±29	78±9
Fe	1340±39	3536±66	3243±64	4945±82	3365±67	1938±47
Zn	ND	32±4	92±6	122±6	54±5	43±4
Sr	55±5	58±5	61±6	51±56	5±6	49±5
Zr	19±4	33±5	35±5	47±62	4±5	15±4

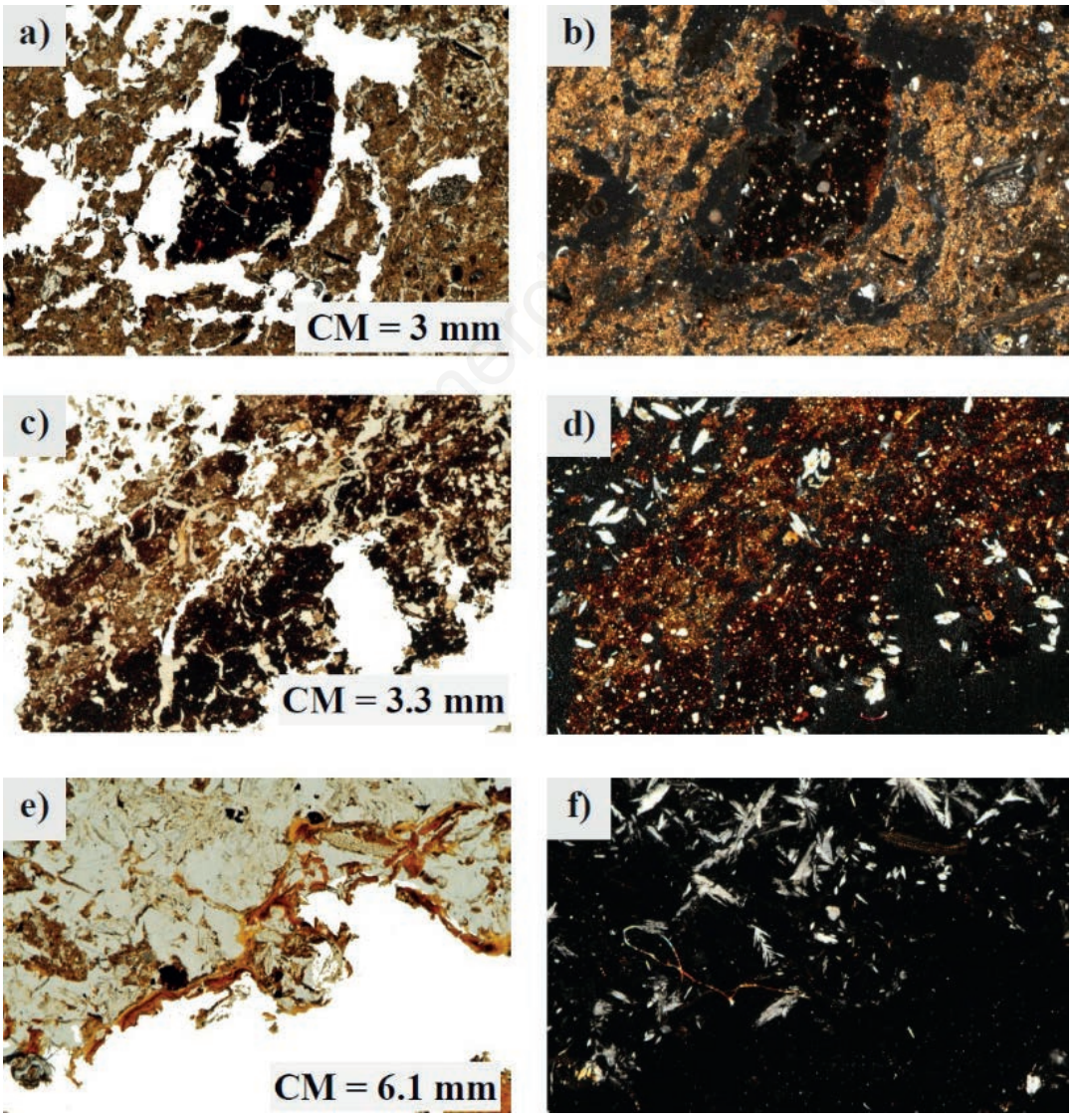

Figure 12. Optical micrographs of selected soil features. a) and b) Blackish aggregate of organic material in carbonate matrix (PPL and XPL, respectively); c) and d) organic material mixed with mineral component (PPL and XPL, respectively); e) and f) organic matter coatings inside a soil pore (PPL and XPL, respectively). PPL, plane polarized light; XPL, crossed polarized light.

Moreover, it is noteworthy that Cr content associated to these sulphate minerals is remarkable (489 mg kg^{-1}).

Conclusions

From the results obtained the geospatial complexity of contaminated sites, along with the complex spatial distribution of contaminants, appears evident. This has to be ascribed to the complex history of the site and type of deposition of pollutant materials.

It is self-evident that, in sites subject to high environmental risk, such site complexity should not be neglected, also given that a large set of proxy technologies (*e.g.* miniaturized sensors) is currently available and can be directly used in the field for precision soil sampling. The correspondence found between hot spots reported in the maps and presence of heavily contaminated materials in field observations (profiles and trenches) showed that it is indeed possible and sustainable to use a powerful approach that integrates various sensors (indirect measurements and direct surveys) to attain detailed geospatial knowledge of contaminated sites and encourage further applications. Moreover, the information thereby obtained can also reduce the number of samples and costs of analysis, and increase the accuracy in delineating site-specific problems (*e.g.* volume of soil contamination). Soil micromorphology application evidenced the presence of: i) organic materials enriched in Cr and surrounded by a carbonate matrix (or mixed with mineral particles) of allochthonous origin; ii) secondary crystalline gypsum minerals showing notable Cr content; and iii) peculiar soil features (such as organic matter coatings) close to the above mentioned organic materials, indicating movement inside pores of colloidal materials. These observations give a picture of the fate of some contaminants, such as the formation of the Cr-associated organic materials and secondary crystalline gypsum, as well as the downward movement of fine particles in depth as PTE carriers.

Finally, we should highlight the urgent need to improve existing legislation, including approaches like that, which we have shown. This would enable both proper characterization of the geography of contamination and hence proper site restoration. Indeed, the proposed approach is economically sustainable and detailed knowledge of contamination geography enables site-specific remediation techniques to be performed, thus avoiding treatment of non-contaminated soils.

It should be also emphasized that indirect techniques enable data to be acquired in a very short time (1 to 3 days' work per technique, for a survey of 6 ha) and can help transform point-based analysis of standard soil observations into information on continuous spatial soil properties. Homogeneous soil property areas can then be identified and studied in detail by direct investigations.

References

Aggelopoulou KD, Wulfsohn D, Fountas S., Gemtos TA, Nanos GD, Blackmore S, 2010. Spatial variation in yield and quality in a small apple orchard. Precis. Agric. 11:538-56.

Aggelopoulou KD, Pateras D, Fountas S, Gemtos TA, Nanos GD, 2011. Soil spatial variability and site-specific fertilization maps in an apple orchard. Precis. Agric. 12:118-29.

De Benedetto D, Castrignanò A, Diacono M, Rinaldi M, Ruggieri S, Tamborrino R, 2013. Field partition by proximal and remote sensing data fusion. Biosyst. Engine. 114:372-83.

Bonfante A, Agrillo A, Albrizio R, Basile A, Buonomo R, De Mascellis R, Gambuti A, Giorio P, Guida G, Langella G, Manna P, Minieri L, Moio L, Siani T, and Terribile F, 2015. Functional homogeneous zones (fHZs) in viticultural zoning procedure: an Italian case study on Aglianico vine. Soil 1:427-41.

Corwin DL, Lesch SM, 2003. Application of Soil Electrical Conductivity to Precision Agriculture: Theory, Principles, and Guidelines. Agron. J. 95:455-71.

da Silva FBV, do Nascimento CWA, Araújo PRM, da Silva FL, Lima LHV, 2017. Soil contamination by metals with high ecological risk in urban and rural areas. Int. J. Environ. Sci. Techn. 14:553-62.

Di Gennaro A, Aronne G, De Mascellis R, Vingiani S, Sarnataro M, Abalsamo P, Cona F, Vitelli L, Arpaia G, 2002. I sistemi di terre della Campania. Monografia e carta 1:250.000, con legenda. S.E.L.C.A., Firenze, pp. 63.

Di Vito MA, Castaldo N, de Vita S, Bishop J, Vecchio G, 2013. Human colonization and volcanic activity in the eastern Campania Plain (Italy) between the Eneolithic and Late Roman periods. Quat. Intern. 303:132-41.

FAO (Food and Agriculture Organization), 2006. Guidelines for Soil Profile Description (Revised), 4th ed. Rome, Italy.

Fiorentino N, Mori M, Cenvinzo V, Duri LG, Gioia L, Visconti D, Fagnano M, 2018. Assisted phytoremediation for restoring soil fertility in contaminated and degraded land. Ital. J. Agron. 13(s1):34-44.

FitzPatrick EA, 1984. Micromorphology of soils. Chapman and Hall, London, pp. 433.

FitzPatrick EA, 1993. Soil Microscopy and Micromorphology. Wiley, West Sussex, England, pp. 304.

Fulton A, Schwankl L, Lynn K, Lampinen B, Edstrom J, Prichard T, 2011. Using EM and VERIS technology to assess land suitability for orchard and vineyard development. Irrig. Sci. 29:497-512.

Mzuku M, Khosla R, Reich R, Inman D, Smith F, MacDonald L, 2005. Spatial Variability of Measured Soil Properties across Site-Specific Management Zones. Soil Sci. Soc. Am. J. 69:1572-9.

Nanzyo M, 2002. Unique properties of volcanic ash soils. Global Environ. Res. 6:99-112.

Orsi G, Di Vito MA, Isaia R, 2004. Volcanic hazard assessment at the restless Campi Flegrei caldera. Bull. Volcan. 66:514-30.

Rocco C, Duro I, Di Rosa S, Fagnano M, Fiorentino N, Vetromile A, Adamo P, 2016. Composite vs. discrete soil sampling in assessing soil pollution of agricultural sites affected by solid waste disposal. J. Geochem. Explor. 170:30-8.

Rocco C, Agrelli D, Tafuro M, Caporale AG, Adamo P, 2018. Assessing the bioavailability of potentially toxic elements in soil: a proposed approach. Ital. J. Agron. 13(s1):16-22.

Santos-Francés F, Martínez-Graña A, Zarza CÁ, Sánchez AG, Rojo PA, 2017. Spatial distribution of heavy metals and the environmental quality of soil in the Northern Plateau of Spain by geostatistical methods. Int. J. Environ. Res. Public Health 14:568.

Shaheen A and Javed Iqbal J, 2018. Spatial Distribution and Mobility Assessment of Carcinogenic Heavy Metals in Soil Profiles Using Geostatistics and Random Forest, Boruta Algorithm. Sustainability 10:799.

Tardaguila J, Diago MP, Priori S, Oliveira M, 2018. Mapping and managing vineyard homogeneous zones through proximal geoelectrical sensing. Archiv. Agron. Soil Sci. 64:409-18.

Vingiani S, Terribile F, Adamo P, 2013. Weathering and particle entrapment at the rock-lichen interface in Italian volcanic envi-

ronments. Geoderma 207-208:244-55.
Vingiani S, Scarciglia F, Mileti FA, Donato P, Terribile F, 2014. Occurrence and origin of soils with andic properties in Calabria (southern Italy). Geoderma 232-4:500-16.
Vingiani S, Mele G, De Mascellis R, Terribile F, Basile A, 2015. Volcanic soils and landslides: A case study of the island of Ischia (Southern Italy) and its relationship with other Campania events. Solid Earth 6:783-97.
Vingiani S, Buonanno M, Coraggio S, D'Antonio A, De Mascellis R, di Gennaro A, Iamarino M, Langella G, Manna P, Moretti P, Terribile F, 2018. Soils of the Aversa plain (southern Italy). J. Maps 14:312-20.
Vingiani S, Minieri L, Albore Livadie C, Di Vito M, Terribile F, 2018. Pedological investigation of an early bronze age site in southern Italy. Geoarchaeol. 33:193-217.
Wang G, Zhang S, Xiao L, Zhong Q, Li L, Xu G, Deng O, Pu Y, 2017. Heavy metals in soils from a typical industrial area in Sichuan, China: Spatial distribution, source identification, and ecological risk assessment. Environ. Sci. Pollut. Res. 24:16618-30.